Physics Procedia

Volume 75, 2015, Pages 284–291

20th International Conference on Magnetism

Development of a rapid temperature scanning system for pulsed magnetic fields and its applications

Kenji MOCHIDZUKI, Yoshimitsu KOHAMA, Akira MATSUO and Koichi KINDO

The Institute for Solid State Physics, the University of Tokyo, Kashiwa, Japan

kmochi@issp.u-tokyo.ac.jp, ykohama@issp.u-tokyo.ac.jp, a-matsuo@issp.u-tokyo.ac.jp, kindo@issp.u-tokyo.ac.jp

Abstract

An apparatus, which scans temperature in sub-seconds for measuring the temperature dependence of the resistivity, is proposed. This apparatus contains a thermal bath and a sample platform on which a thin-film thermometer and a thin-film heater are sputtered. By thermally isolating the sample platform from surrounding parts, the sample temperature can be scanned at a high sweep rate of 200-300 K/s. As a demonstration of the apparatus, the resistivity of a niobium-titanium alloy is measured in a pulsed magnetic field. In addition, as another application of the apparatus, the dielectric polarization measurement of the quantum-paraelectric material $SrTiO_3$ is described.

Keywords: Pulsed magnet, Temperature scanning measurement, Resistivity, Dielectric polarization

1 Introduction

Pulsed magnets enable to generate magnetic fields higher than 50 T. In pulsed magnetic fields, owing to theirs high field scanning rate, high-resolution polarization and magnetization measurements have been done. By contrast, because of the short pulse duration, it is difficult to measure the temperature dependences of the specific heat and so on. Recently, to overcome this problem, long pulse magnetic fields with duration times over 1 s have been developed. Jaime *et al*. have succeeded in measuring the temperature dependence of the specific heat in long-pulsed magnetic fields with sub-seconds flat region around the top of the field (flat-top magnetic field) in 2000. [1] On the other hand, Weickert *et al*. have also measured the specific heat around the top of 1.5 s long-pulsed magnetic fields in 2012. [2] More recently, the technique of thin-film fabrication has been improved and thin-film thermometers and thin-film heaters have been sputtered on samples directly. By using this technique, the specific heat has been measured around the top of 36 ms pulsed magnetic field. [3]

Selection and peer-review under responsibility of the Scientific Programme Committee of ICM 2015

doi:10.1016/j.phpro.2015.12.033

However, the temperature dependence of the physical properties that can be measured in pulsed magnetic fields is limited to the specific heat.

In this paper, we introduce an apparatus, which enables to sweep temperature in sub-seconds. To demonstrate the performance of the apparatus, resistivity measurements of the superconducting niobium-titanium (NbTi) alloy in a pulsed magnetic field is reported. Moreover, the dielectric polarization measurement of $SrTiO_3$ is presented as another application of this apparatus.

2 Method

In order to perform a temperature sweep measurement in a short time duration, it is necessary to thermally isolate a sample platform from the surrounding parts. The platform ideally equips both heater and thermometer that should be thermally well coupled to the sample. Such a device is known as a heat pulse calorimeter. [4] Figure 1 shows the design of the apparatus, which we propose for sweeping the sample temperature in a short time-period. The apparatus consists of a thermal bath, a sample platform on which a thin film thermometer and a thin film heater are directly sputtered. To avoid eddy-current heating, the thermal bath is made of a single crystalline-quartz, and a single crystalline-sapphire is used as the sample platform. The sample platform is connected with the thermal bath with constantan wires of 50 μm diameter (ϕ50 μm) for thermally isolating from surrounding parts. These constantan wires also give the electric passes to the thermometer and heater. An $Au_{0.18}Ge_{0.82}$ (AuGe), which has a high sensitivity (dR/dT = 0.3-5 kΩ/K [3.5]) below 100 K is used as a thin-film thermometer. For a thin film heater, we use a $Ni_{0.50}Cr_{0.50}$ (NiCr) thin film, which shows both small temperature and magnetic field dependences of the resistivity. [3] The sample is attached to the platform with insulating GE-vernish. For the resistivity measurement, four constantan wires of ϕ25 μm are connected to the sample with silver paste (DuPont 4922N). The sample resistance is measured by the four-probe method for removing the contact resistance. The resistances of the sample and thermometer are measured by using AC currents of 2 kHz.

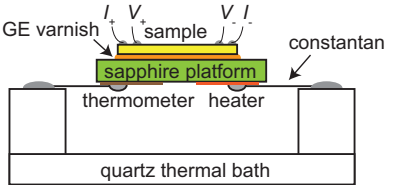

Figure 1: Design of the apparatus for rapid temperature scanning measurement

To assess the accuracy in the temperature measurement, we theoretically investigate the heat flow model for this apparatus shown in Fig. 2. Here we denote the heat capacities of the sample and the platform as C_s and C_p, respectively. The temperatures of the sample, sample platform and thermal bath are defined as T_s, T_p and T_b, respectively. Moreover the thermal conductance between each pairs of the calorimeter components is written as $K_{x\text{-}y}$, where x and y represent the sample (s), thermal bath (b) and platform (p), respectively. In this model, we neglect the specific heats and the thermal couplings of thermometer and heater, since our apparatus employs a thin-film thermometer and a thin-film heater.

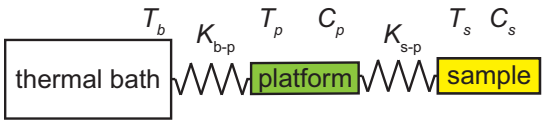

Figure 2: Thermal flow model of heat-pulse calorimeter

The heat flow model in Fig. 2 can be formalized by the following equations, [6]

$$C_{\mathrm{s}}\frac{dT_{\mathrm{s}}}{dt} = K_{\mathrm{s-p}}\left(T_{\mathrm{p}} - T_{\mathrm{s}}\right) \tag{2.1}$$

$$C_{\mathrm{p}}\frac{dT_{\mathrm{p}}}{dt} = K_{\mathrm{s-p}}\left(T_{\mathrm{s}} - T_{\mathrm{p}}\right) + K_{\mathrm{b-p}}\left(T_{\mathrm{b}} - T_{\mathrm{p}}\right) + P(t). \tag{2.2}$$

Assuming the heat power $P(t)$ has a square pulsed form, it is given by

$$P(t) = \begin{cases} P & (\text{turn on heater}) \\ 0 & (\text{turn off heater}). \end{cases} \tag{2.3}$$

It is well known that the general solutions for T_{p} and T_{s} are written as followings,

$$T_p(t) = a_1 e^{-\frac{t}{\tau_1}} + a_2 e^{-\frac{t}{\tau_2}} + \frac{P}{K_{b-p}} + T_b \tag{2.4}$$

$$T_s(t) = a_1 b_1 e^{-\frac{t}{\tau_1}} + a_2 b_2 e^{-\frac{t}{\tau_2}} + \frac{P}{K_{b-p}} + T_b. \tag{2.5}$$

Both T_{p} and T_{s} contain multiple exponential functions, where each exponential function has a different time parameter, τ_1 or τ_2. The parameters are called as thermal time constants, which are given by

$$\tau_{1,2} = \frac{1}{2K_{b-p}K_{s-p}}\left[(C_s+C_p)K_{s-p} + C_s K_{b-p} \pm \sqrt{\left\{(C_s+C_p)K_{s-p} + C_s K_{b-p}\right\}^2 - 4C_s C_p K_{b-p} K_{s-p}}\right], \tag{2.6}$$

where the signs, plus and minus in front of the square root, refer to τ_1 and τ_2, respectively. The longer time constant, τ_1, indicates the thermal relaxation time between the sample and the thermal bath, and it corresponds to the time scale of temperature sweep. In contrast, the shorter time constant τ_2 is the thermal response time between the sample and the sample platform. The pre-exponential factors of the equations (2.4) and (2.5) are determined from the initial condition $T_{\mathrm{p}}(0) = T_{\mathrm{s}}(0) = T_{\mathrm{b}}$, which are written as

$$a_{1,2} = \frac{P}{K_{b-p}(\tau_{1,2} - \tau_{2,1})}\left(\frac{C_s}{K_{s-p}} - \tau_{1,2}\right) \tag{2.7}$$

$$b_{1,2} = 1 + \frac{K_{b-p}}{K_{s-p}} - \frac{C_p}{K_{s-p}\tau_{1,2}}. \tag{2.8}$$

To assess the correctness of the measurement of the sample temperature, we define the temperature difference between the sample and the sample platform as $T^{\mathrm{error}} = T_{\mathrm{p}} - T_{\mathrm{s}}$, which can be written as

$$T^{\mathrm{error}} = T_p - T_s = a_1(1-b_1)\left(e^{-\frac{t}{\tau_1}} - e^{-\frac{t}{\tau_2}}\right). \tag{2.9}$$

T^{error} contains multiple exponential functions similar to T_{p} and T_{s}. Since the first term of the right-hand side of the equation (2.9) is the exponential function with time constant τ_1 same as the time scale of the temperature scanning, the coefficient $a_1(1-b_1)$ must be minimized for decreasing the contribution of this term. In contrast, the second term of the right-hand side of the equation (2.9) has a large value in a short time just after a heat-pulse is applied and removed because it represented the exponential function with short time constant τ_2. Thus in order to reduce the contribution of the second term, the minimizing time constant τ_2 is effective method. To simplify, we assume that the sample platform is well isolated from the thermal bath ($K_{\mathrm{s-p}}/K_{\mathrm{b-p}} >> 1$). In this condition, $a_1(1-b_1)$ and τ_2 are approximated as followings,

$$\tau_2 \sim \frac{C_p}{K_{s-p}}\left(\frac{C_s}{C_s + C_p}\right) \tag{2.10}$$

$$a_1(1-b_1) \sim \frac{PK_{b-p}}{{K_{s-p}}^2}\left(\frac{C_s}{C_s + C_p}\right). \tag{2.11}$$

In order to decrease these values simultaneously, we consider the condition for minimizing the common part of equations (2.10) and (2.11), $C_s/(C_s+C_p)K_{s-p}$. This part decreases monotonically as reducing of the C_s or increasing of the C_p and K_{s-p}. However, the increasing of the C_p leads the large τ_1, i.e. the temperature cannot be scanned at a high rate. In addition, the large K_{s-p} cannot be expected in the case of the resistivity measurement because we cannot use any electrically conductive material to attach the sample on the platform. Therefore, the decreasing of the heat capacity of the sample C_s is necessary to reduce the T^{error}, namely to do the temperature scanning measurement in a short time duration.

We used a commercially available polycrystalline NbTi alloy. The NbTi alloy is a suitable material to verify the accuracy of the temperature measurement because it shows the very sharp resistance step at the superconducting transition temperature T_c. A plate-shaped NbTi sample was obtained by pressing the NbTi wire of 62 μm in a press machine to get the heat capacity small. The resultant size of the NbTi sample was 1.8×0.080×0.021 mm^3 and its mass and heat capacity were about 0.080 mg and 0.066 μJ/K [7], respectively

We used the flywheel generator (210 MJ, 51.3 MW) and 1.3 s long-pulsed magnet at the Institute for Solid State Physics (ISSP), the University of Tokyo. This magnet can generate magnetic fields up to 36 T, 500 ms flat-top magnetic fields below 20 T and 100-200 ms flat-top magnetic fields over 20 T.

3 Results and discussions

3.1 Resistivity measurement

Figure 3(a) shows the result of resistivity measurement in NbTi alloy under zero magnetic field. Here black, blue and red lines in Fig. 3(a) correspond to the time dependences of the sample resistance, sample temperature and temperature sweep rate, respectively. The dashed lines indicate the time at which the sample heater is turned on or off. At the moment that heat power was applied, the temperature sweep rate reached to 3000 K/s, but rapidly dropped to 200-300 K/s after a few milliseconds. After turning off the heater, the sample temperature was decreased at the rate of −200-300 K/s and gradually reached to the base temperature (1.8 K) in 60 ms. Because of the temperature dependence of the specific heat, $T(t)$ curve did not obey a multi-exponential form given by equation (2.4). However, the obtained result implies, at least, that the τ_1 is less than 60 ms below 20 K, and another thermal relaxation process caused by the second (τ_2) term in equation (2.4) was not obvious in this time resolution (0.5 ms of 2 kHz measurement), suggesting $\tau_2 <\sim 0.5$ ms. The sample resistance shows the step-like behaivor at 9.2 K in both warming and cooling process.

As shown in Fig. 4, these data are compared with that measured by Quantum Design Physical Property Measurement System (PPMS), where black line is the resistivity measured by PPMS, and the red triangles and blue circles are the temperature dependences of resistivity data obtained in a heating and a cooling curves of Fig.3 (a), respectively. In spite of a high temperature sweep rate of 200-300 K/s, the result shows an excellent agreement with that measured by using PPMS, which indicates that no T^{error} is observed in our resolution of temperature measurement. This agreement can be considered to be achieved since the small heat capacity of NbTi sample (C_s) leads small a_1 ($1-b_1$) and τ_2 in equation (2.9). In fact, the value of the a_1 ($1-b_1$) and τ_2 in our apparatus can be estimated as 12 mK and 0.12 ms, respectively. Indeed, these errors cannot be observed in our system. From these facts, we can conclude that our apparatus enables to measure the temperature dependence of the resistivity in a short time ~120 ms. This is shorter than the time scale of the flat-top magnetic field generated at ISSP, the University of Tokyo.

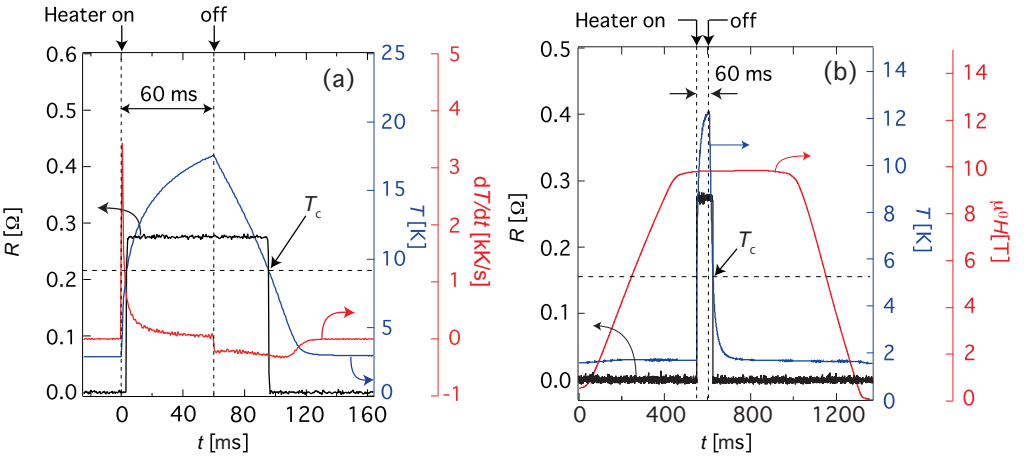

Figure 3: (a) Result of a resistivity measurement without magnetic field, black, blue and red lines indicate the time dependences of the resistance, temperature and temperature sweep rate, respectively. (b) Result of the resistivity measurement for the flat-top magnetic field of 10 T, black, blue and red lines denote the time dependences of resistance, temperature and magnetic field applied to the sample, respectively.

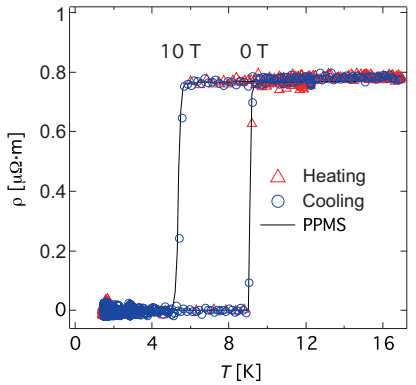

Figure 4: Resistivity of Nb-Ti at 0 T and 10 T plotted against temperature, black line shows the resistivity measured by PPMS, and red triangles and blue circles show the resistivity measured in heating and cooling process by using our system, respectively.

Next, the result of the resistivity measurement in a 500 ms flat-top magnetic field at 10 T is shown in Fig. 3(b). In this figure, the black, blue and red curves denote the sample resistance, temperature and magnetic field applied to the sample, respectively. The magnetic field had a total duration of 1.3 s and a flat-top region of 500 ms. In this flat-top region, a 60 ms heat pulse was applied to the sample, and the sample temperature was swept from 1.8 K to 12 K. The critical temperature of superconducting transition is suppressed to 5.4 K by the magnetic field. The observed temperature dependence of the resistivity is compared with data measured in PPMS as plotted in Fig. 4. The critical temperature at the superconducting phase transition clearly agreed with the result obtained by PPMS (T_c=5.4± 0.05 K), and the overall temperature dependence including the absolute value of resistivity again showed a good agreement.

To compare the method proposed in this paper to classical method in pulsed magnetic fields, our apparatus can improve the accuracy and resolution of the temperature measurement significantly. Even if eddy current heating caused by rapid sweeping of the magnetic field changes the sample temperature, our apparatus can observe it, since the relaxation time between the sample and sample platform in this apparatus (~0.1 ms) is much shorter than the time scale of the long pulsed magnetic fields (>1 s). In addition, by using the heater on the platform, the sample temperature can be swept in

sub-seconds flat-top magnetic fields. In our method, the temperature resolution of the resistivity is given by the product of the temperature-scanning rate (200-300 K/s) and the measurement interval (0.5 ms). Thus our apparatus can measure the temperature dependence of the resistivity with a high temperature resolution of 0.10-0.15 K in a wide temperature range between 1.8 and 20 K. Although, in this paper, the result of the resistivity measurement of superconducting Nb-Ti is reported, this method will be applied to other metals such as the strongly correlated materials, which show a complex temperature dependence of the resistivity or other measurements (polarization, magnetization and so on). Finally, to demonstrate an application of our apparatus, we present polarization measurements of the quantum paraelectric $SrTiO_3$, which has a very large temperature dependence of the dielectric constant $d\varepsilon/dT$.

3.2 Dielectric polarization measurement

The pyroelectric current i_{pyro} can be observed when the dielectric polarization P is changed by the temperature change. The magnitude of the i_{pyro} is written as following

$$i_{pyro} = S\frac{dP}{dt} = S\frac{dP}{dT}\frac{dT}{dt}, \qquad (4.1)$$

where S denotes the area in which the pyroelectric current is detected. From this equation, we can consider that a rapid temperature sweeping is necessary to increase the magnitude of the i_{pyro}. To integrate the equation (4.1), the polarization ΔP is given as

$$\Delta P = P(T) - P(T_{base}) = \frac{1}{S}\int_{T_{base}}^{T} i_{pyro}\, dt. \qquad (4.2)$$

Thus, the i_{pyro} gives us the ΔP from a base temperature.

The photo of the apparatus for measuring the pyroelectric current i_{pyro} is shown in Fig. 5(a). This apparatus contains a thermal bath and the sample ($SrTiO_3$) on which a thin-film AuGe thermometer and a thin-film NiCr heater are directly sputtered. To sweep the sample temperature rapidly, the sample is hung by using ϕ50 μm constantan wires, and thermally isolated from the thermal bath. In order to detect the i_{pyro} from the sample, Au thin-films are sputtered both side of the sample, and electrically connected with ϕ50 μm constantan wires. The sample used in this experiment was (100) oriented $SrTiO_3$ and its cross section area was 3.5×2.9 mm^2 shown in Fig. 5 (a) and thickness was 75 μm. The area of sputtered Au thin-film was 2.4×2.2 mm^2. Figure 5(b) shows the electric circuit for the pyroelectric measurement. To induce a polarization of paraelectric $SrTiO_3$, a 9.3V battery is connected to the sample and thereby an electric field of 120 kV/m is applied between Au thin-films. The pyroelectric current is detected by using a shunt resistor of 10 kΩ, and the signal is digitized after amplification.

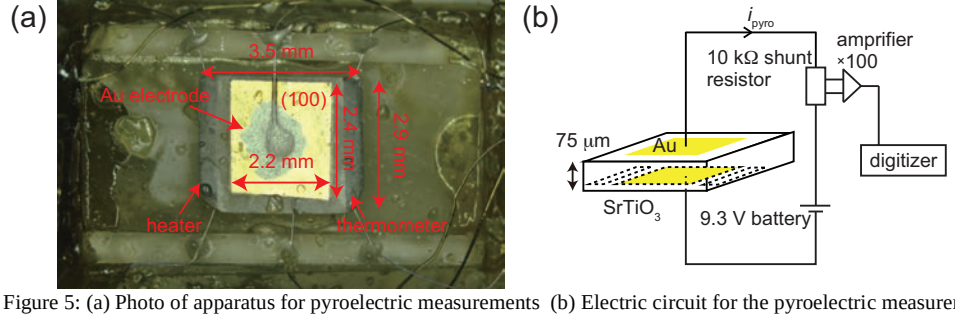

Figure 5: (a) Photo of apparatus for pyroelectric measurements (b) Electric circuit for the pyroelectric measurement

Figure 6(a) shows the result of the pyroelectric current measurement. In upper panel, black and red lines denote the time dependences of the pyroelectric current i_{pyro} and heat power P, respectively. In lower panel black and red lines indicate the time dependences of the temperature T and heat power P,

respectively. A 50 ms heat pulse (~4 mW) was applied, and sample temperature rose up to 24 K from the base temperature 6.8 K. Just after heat pulse was removed, a rapid relaxation between sample and thermometer was observed. This suggests that the error in temperature measurement is large during the heat pulse is applied and just after heat pulse is turned off. The observable i_{pyro} was induced by the temperature sweeping and took maximum value ~80 nA at the moment that the heat-pulse is applied. The value of the i_{pyro} was declined since temperature sweep rate reduced. After the heat pulse was removed, the temperature decreased slowly because of the well thermal isolation and the value of the i_{pyro} was ~10 nA. In Fig. 6 (b) the polarization difference ΔP from base temperature given from the integration of the i_{pyro} is plotted against temperature. In this figure, the red curve denotes the ΔP given from the integration of the i_{pyro} in Fig. 6 (a) and the blue curve indicates the ΔP induced by a weaker heat pulse (~1 mW). Because of the τ_2 effect, the reproducible results could not be observed in warming process and just after the heat power was removed. However, in cooling process after τ_2 relaxation, we obtained the well reproducible results. Therefore, we considered the result in cooling process is the temperature dependence of the polarization of the $SrTiO_3$. The polarization decreased by -0.54 mC/m^2 from 6.8 K to 23 K. We can calculate the difference of the dielectric constant $\Delta\varepsilon$ as −500 from this polarization difference ΔP. This value is 10 times smaller than that reported by Bednorz[8]. This may be caused by the impurity effect since the dielectric constant of $SrTiO_3$ can be changed significantly by a few impurities. [8-10]

Our apparatus can be used for polarization measurements of dielectrics. A very small pyroelectric current of 10-80 nA was observed, even though the $SrTiO_3$ was used as the test sample. Therefore, in order to apply to a number of materials, which have a $d\varepsilon/dT$ much smaller than that of $SrTiO_3$, the apparatus for rapid temperature sweeping proposed in this paper is essential.

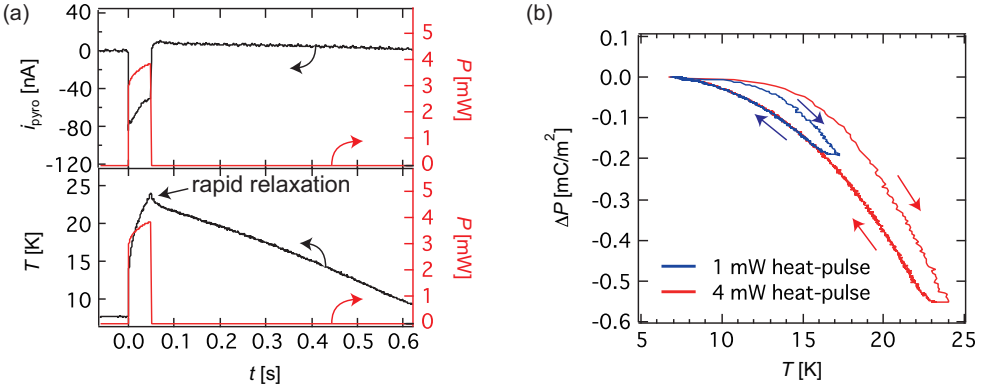

Figure 6: (a) Time dependent of the pyroelectric current (black curve in the upper panel) and temperature (black curve in the lower panel). The hater power is denoted by red curve in both upper and lower panel (b) Temperature dependences of the polarizaion of the $SrTiO_3$; the red and blue curve shows the results in the case of 4mW and 1mW heat-pulse, respectively.

4 Conclusion

We developed an apparatus that enables to do temperature-scanning measurement in sub-seconds. From the resistivity measurement of the NbTi alloy, this apparatus can sweep the sample temperature at a high rate of 200-300 K/s, and we succeeded in measuring the temperature dependence of the resistivity in 120 ms. Moreover, we did same measurement in a 500 ms flat-top magnetic field and got results which showed good agreement with that measured in a static magnetic field. Moreover, this apparatus was used for dielectric polarization measurements on $SrTiO_3$.

5 Acknowledgements

We would like to thank to Y. Hashimoto and Prof. S. Katsumoto at the Institute for Solid State Physics, the University of Tokyo for the thin-film fabrication.

References

[1] M. Jaime *et al*., Nature **405**, 160-163 (2000).

[2] F. Weickert *et al*., Meas. Sci. Technol. **23**, 105001 9pp (2012).

[3] Y. Kohama *et al*., Meas. Sci. Technol. **24,** 115005 (2013).

[4] R. Bachmann *et al*., Rev. Sci. Instrum. **43**, 205 **(**1972**)**.

[5] T. Kihara *et al*., Rev. Sci. Instrum. **84**, 074901 (2013).

[6] H. Wilhelm *et al*., Rev. Sci. Instrum. **75**, 2700 (2004).

[7] Thomas P. Sheahen: *Introduction to High-Temperature Superconductivity* (Plenum Press, New York) p. 351(1994).

[8] J. G. Bednorz *et al*., Phys. Rev. Lett. **52**, 2289 (1984).

[9] J. F. Schooley *et al*., Phys. Rev. Lett. **12**, 474 (1964).

[10] H. Takashima *et al*., Appl. Phys. Lett. **88**, 082906 (2006).